Phonons and librons in nitrogen monolayers adsorbed on graphite

T. H. M. van den Berg and A. van der Avoird
Institute of Theoretical Chemistry, University of Nijmegen, Toernooiveld, 6525 ED Nijmegen, The Netherlands
(Received 21 December 1990)

For the ordered commensurate and incommensurate N_2 monolayers that are formed at low T on the basal plane of graphite, we have calculated the structure and lattice dynamics by means of the quantum-mechanical mean-field and time-dependent Hartree methods. The potential used is an *ab initio* potential for the N_2-N_2 interactions, with its anisotropy expanded in spherical harmonics, and an empirical atom-atom potential for the N_2-graphite interactions, with variable parameters. The molecular center-of-mass vibrations are expanded in three-dimensional harmonic-oscillator functions and the librations in a free-rotor basis; translation-rotation coupling is explicitly included. We discuss the anharmonic shifts in the frequencies of the in-plane and out-of-plane phonons and librons, but we find that these shifts, with the exception of the soft out-of-plane libration in the compressed incommensurate herringbone phase, are not larger than in bulk nitrogen in the ordered α and γ phases. For the incommensurate monolayer, we find at zero pressure that the planar herringbone ordering, which occurs also in the commensurate phase, is more stable than the pinwheel structure. At higher pressures, but probably still before bilayer formation, the pinwheel structure seems to be more stable, however. For the commensurate monolayer we obtain good agreement with the phonon frequencies from inelastic neutron scattering, except for the acoustic-phonon gap. Since this gap is directly related to the corrugation in the N_2-graphite potential, we must conclude that this corrugation cannot be correctly reproduced by an atom-atom model, even when the parameters are varied within reasonable limits.

I. INTRODUCTION

Physically adsorbed layers of N_2 molecules on graphite occur in a variety of quasi-two-dimensional phases. Of basic interest are the stability and dynamics of these phases, the transitions between them and the way in which their behavior depends on the intermolecular and molecule-substrate interactions. Especially over the last few years a number of experimental and theoretical studies have appeared. Structures and phase transitions have been characterized by neutron, x-ray, and low-energy-electron diffraction and by specific-heat measurements.[1–12] The adlayer dynamics has been investigated recently by inelastic neutron scattering[13–15] and, in the near future, will be studied probably in more detail by inelastic helium scattering.[16–18] Theoretical investigations have started from empirical-model potentials; they involve static potential-energy calculations[19] and the use of harmonic[15,20–22] or quasiharmonic[23] lattice dynamics and classical Monte Carlo[24–28] or molecular-dynamics[21,29–31] (MD) methods. An excellent review of the results that have been obtained from these studies is given in the recent paper by Roosevelt and Bruch.[23]

In the present paper we concentrate on the commensurate $(\sqrt{3}\times\sqrt{3})R30°$ monolayer for which the most experimental data are available, and on the incommensurate monolayers. These phases are orientationally ordered and stable at low temperature, for lower and higher coverages, respectively. For the $(\sqrt{3}\times\sqrt{3})R30°$ phase a herringbone ordering of the N_2 molecules is well established.[6,8,11] Also the uniaxially incommensurate phase has the herringbone structure, but for the so-called triangular incommensurate phase that occurs at higher pressures both a herringbone and a pinwheel structure are still considered possible.[8,10,32] We study the dynamics of these phases; the (theoretical) method that we use for this purpose is in several respects complementary to the (quasi)harmonic and classical MD methods used before.[15,20–23,29–31]

The pair potential assumed between the N_2 molecules in the adsorbed layer originates directly from *ab initio* calculations.[33] It is not fitted to a site-site model as used in the other calculations,[19–31] but instead its anisotropy is explicitly expressed by a converged expansion in spherical harmonics.[34] In recent work on solid nitrogen[35–39] it has been confirmed that this representation of the orientational dependence of the potential is essential for obtaining accurate librational frequencies. With a site-site model fitted to the same *ab initio* data the librational frequencies in solid α-N_2 and γ-N_2 are 30% too high. The use of this anisotropic expansion of the potential implies that the molecular quadrupole and higher multipole interactions are exactly included, without recourse to a point-charge model. For the molecule-substrate interactions we use the same empirical atom-atom potential of Steele[40] that was used in other calculations.[19–31] Because of the uncertainty in these interactions we apply a systematic variation of the parameters in this potential.

The method that we use to perform the lattice-dynamics calculations is the time-dependent Hartree (TDH) method.[37,41] At zero temperature this method is equivalent to the random-phase approximation (RPA). It

is also equivalent to the susceptibility approach[42–44] which has been used for the (semiempirical) description of orientational order-disorder phase transitions. In our group this method has been extended in order to include the anharmonic center-of-mass vibrations of the molecules, which are expanded in a basis of three-dimensional harmonic-oscillator wave functions. The librational wave functions are expanded in spherical harmonics and the effects of rotation-translation coupling are explicitly taken into account. As illustrated by applications to solid α and γ nitrogen[35–39] this method is suitable for the calculations of motions with larger amplitudes. The anharmonic effects enter in two ways. First, there is a dilation of the lattice by the averaging over the (zero-point or temperature) vibrations of the molecules in the anharmonic potential wells. This effect, which leads in general to a downward shift of the frequencies, is also included in the quasiharmonic theory. In commensurate overlayers it cannot occur in the directions parallel to the surface, but in the perpendicular direction it is expected to be rather important.[45] Secondly, there is a direct effect of the (mainly cubic and quartic) anharmonic terms in the potential, which leads to an upward shift of the frequencies in bulk nitrogen.[39] Classical MD calculations[21] indicate that these anharmonic effects are larger for adsorbed layers than they are in bulk solids. On the other hand, our TDH study is complementary to the classical MD treatments[21,29–31] in that it includes the quantum-mechanical zero-point vibrations and librations which reduce the cohesion or adsorption energies in these systems[46–48] by about 15%. This is essential in considerations about phase stability.

II. FORMALISM

A. The Hamiltonian

The center-of-mass positions of the molecules in the adsorbed layer are denoted by $\mathbf{r}_p=\mathbf{R}_p+\mathbf{u}_p$, where $\mathbf{R}_p$ are the equilibrium positions and $\mathbf{u}_p$ the displacements of the molecules p. The orientations of the molecules are described by a set of polar angles ω_p. We assume that the motions of the molecules in the adsorbed layer are separable from the graphite lattice vibrations which have much higher frequencies and small amplitudes. We use a rigid graphite substrate, so that the molecule-substrate potential V_p for a given molecule p depends only on the coordinates $\mathbf{u}_p$ and ω_p of that molecule. The pair potential between the molecules within the adsorbed layer is denoted by $\Phi_{pp'}$. Many-body interactions, as well as substrate-mediated interactions between the adsorbed molecules, are neglected. Then, the Hamiltonian for the adsorbed layer is given by

$$H=\sum_p T(\mathbf{u}_p)+\sum_p L(\omega_p)+\sum_p V_p(\mathbf{u}_p,\omega_p)+\tfrac{1}{2}\sum_p\sum_{p'\neq p}\Phi_{pp'}(\mathbf{u}_p,\omega_p,\mathbf{u}_{p'},\omega_{p'}) . \quad (1)$$

It contains the kinetic-energy terms for the translational center-of-mass motions T and the rotational motions L of the molecules, the molecule-substrate potential V_p and the intermolecular potential $\Phi_{pp'}$.

The anisotropic intermolecular potential is written in the form of a spherical expansion[34]

$$\Phi_{pp'}(\mathbf{u}_p,\omega_p,\mathbf{u}_{p'},\omega_{p'})=\sum_l \varphi_l(r_{pp'})\sum_{\mathbf{m}}\begin{pmatrix} l_1 & l_2 & l_3 \\ m_1 & m_2 & m_3\end{pmatrix} C_{m_1}^{(l_1)}(\omega_p)\times C_{m_2}^{(l_2)}(\omega_{p'})C_{m_3}^{(l_3)}(\hat{\mathbf{r}}_{pp'}) . \quad (2)$$

The intermolecular vector is given by $\mathbf{r}_{pp'}=(\mathbf{R}_{p'}+\mathbf{u}_{p'})-(\mathbf{R}_p+\mathbf{u}_p)$ and $\hat{\mathbf{r}}_{pp'}$ is the unit vector along $\mathbf{r}_{pp'}$. The Racah spherical harmonics $C_m^{(l)}(\omega)$ that describe the orientational dependence of the potential are coupled to a scalar function by the summation over $\mathbf{m}=\{m_1,m_2,m_3\}$, with the large parentheses denoting a 3-j symbol.[49] The first summation runs over $l=\{l_1,l_2,l_3\}$ and the factors $\varphi_l(r_{pp'})$ are the expansion coefficients that reflect the anisotropy of the potential. Each expansion coefficient $\varphi_l(r)$ consists of dispersion contributions ($\sim r^{-6}$, r^{-8}, and r^{-10}) and short-range contributions, which depend exponentially on r. The quadrupole-quadrupole interaction ($\sim r^{-5}$) appears in the $l_1,l_2,l_3=2,2,4$ term and the higher multipole interactions ($\sim r^{-l_3-1}$) in the other terms with $l_1+l_2=l_3$. The parameters in all these contributions have been directly obtained from *ab initio* calculations on the N_2-N_2 dimer.[33] The expansion appears to be converged for $l_1,l_2\leq 6$ with $l_1+l_2\leq 10$.

The potential as written in Eq. (2) depends on the molecular center-of-mass displacements $\mathbf{u}_p$ and $\mathbf{u}_{p'}$ through the intermolecular vector $\mathbf{r}_{pp'}$. Its dependence on $\mathbf{u}_p$ and $\mathbf{u}_{p'}$ can be made explicit by a double Taylor expansion.[37] In Appendix A we describe a more efficient expansion in $\mathbf{u}_{p'}-\mathbf{u}_p$ which leads to essentially the same result

$$\Phi_{pp'}(\mathbf{u}_p,\omega_p,\mathbf{u}_{p'},\omega_{p'})=\sum_{\Lambda_1}\sum_{\Lambda_2}(u_p)^{\alpha_1}C_{\mu_1}^{(\lambda_1)}(\hat{\mathbf{u}}_p)C_{m_1}^{(l_1)}(\omega_p)\times X_{\Lambda_1\Lambda_2}(\mathbf{R}_{pp'})(u_{p'})^{\alpha_2}C_{\mu_2}^{(\lambda_2)}(\hat{\mathbf{u}}_{p'})C_{m_2}^{(l_2)}(\omega_{p'}) , \quad (3)$$

where $\mathbf{u}_p=(u_p,\hat{\mathbf{u}}_p)$ are the displacement vectors in polar coordinates and the label Λ stands for the set of the indices $\{\alpha,\lambda,\mu,l,m\}$. The expression for $X_{\Lambda_1\Lambda_2}(\mathbf{R}_{pp'})$ which is given in Appendix A is much faster to evaluate than the expression in Ref. 37. The summation over α_1 and α_2 extends to $\alpha_1+\alpha_2\leq\alpha_{\max}$, where $\alpha_{\max}$ is equal to the order of the Taylor expansion in the displacements. An expansion with $\alpha_{\max}=2$, for instance, yields a potential $\Phi_{pp'}$ which is harmonic in the center-of-mass displacements $\mathbf{u}_p$ and $\mathbf{u}_{p'}$. In the present calculations we carry this expansion up to $\alpha_{\max}=4$ inclusive. For the summations over λ and μ the following holds: $0\leq\lambda_i\leq\alpha_i$ and $-\lambda_i\leq\mu_i\leq\lambda_i$, where λ_i has the same parity as α_i. After this expansion

we have a pair potential which is explicitly dependent on the displacement coordinates of the molecules and thus easy to use in lattice-dynamics calculations.

The interaction V_p of a molecule p with the substrate is considered as a sum of pair interactions between the molecule and the individual substrate atoms. The most general form for such molecule-atom interactions is of course a spherical expansion, i.e., a special case of Eq. (2). We model this interaction by the atom-atom model

$$V_p(\mathbf{u}_p,\omega_p)=\sum_C \{v[|\mathbf{R}_p+\mathbf{u}_p+\mathbf{a}(\omega_p)-\mathbf{R}_C|] + v[|\mathbf{R}_p+\mathbf{u}_p-\mathbf{a}(\omega_p)-\mathbf{R}_C|]\} , \quad (4)$$

where the vectors $\mathbf{R}_C$ denote the positions of the carbon atoms C in the substrate and the orientation dependent vectors $\mathbf{a}(\omega_p)$ describe the positions of the nitrogen atoms with respect to the N_2 center of mass. Just as in the previous calculations[19-31] we choose an atom-atom potential $v(|\mathbf{r}|)$ of the Lennard-Jones type as parametrized by Steele,[40] but we investigate systematically the effects of the variation of these parameters (see Sec. III).

In Ref. 50 it is shown that the atom-atom interactions can be summed to an atom-substrate interaction with the aid of an analytical Fourier transformation. Next, a spherical expansion of the molecule-substrate interaction can be made to expose its anisotropy explicitly and, finally, a molecular-displacement expansion of the spherical expansion is used to make the molecular-substrate potential explicitly dependent on the displacement coordinates of the molecule.[45] Thus we have obtained the molecule-substrate potential in the following form:

$$V_p(\mathbf{u}_p,\omega_p)=\sum_\Lambda F_\Lambda(\mathbf{R}_p)(u_p)^\alpha C_\mu^{(\lambda)}(\hat{\mathbf{u}}_p)C_m^{(l)}(\omega_p) , \quad (5)$$

where again Λ indicates the set of indices $\{\alpha,\lambda,\mu,l,m\}$. The coefficients $F_\Lambda(\mathbf{R}_p)$ can be written as a two-dimensional Fourier series

$$F_\Lambda(\mathbf{R}_p)=\sum_{\mathbf{g}} \bar{F}_\Lambda(\mathbf{g}|z_p)\exp(i\mathbf{g}\cdot\tau_p) , \quad (6)$$

with τ_p denoting the projection of $\mathbf{R}_p$ on the graphite basal plane (the xy plane), so that $\mathbf{R}_p=\tau_p+z_p\mathbf{e}_z$. The vector $\mathbf{g}$ is a vector in the two-dimensional reciprocal lattice of a substrate layer. Analytical expressions for the expansion coefficients $\bar{F}_\Lambda(\mathbf{g}|z_p)$ are given in Ref. 45. The terms with $\mathbf{g}=\mathbf{0}$ describe the flat (but anisotropic and anharmonic) potential which depends only on the height z_p of the molecules above the graphite surface; the terms with $\mathbf{g}\neq\mathbf{0}$ contain the effects of the surface corrugation.

In order to summarize the result of these manipulations we introduce the notion of dynamical variables.[42,43] In the harmonic method these are the center-of-mass displacements and the infinitesimal (linearized) angular displacements of the molecules. In our treatment the dynamical variables are

$$Q_p^{k,\nu}=\begin{cases} C_m^{(l)}(\omega_p) & \text{with } \nu=\rho=(l,m) \text{ for the molecular rotations } (k=r) \\ (u_p)^\alpha C_\mu^{(\lambda)}(\hat{\mathbf{u}}_p) & \text{with } \nu=\tau=(\alpha,\lambda,\mu) \text{ for the center-of-mass vibrations } (k=t) \end{cases} \quad (7)$$

and the lattice Hamiltonian for the adsorbed molecular layer can be written as

$$H=\sum_{p,k} T_p^k+\sum_p\sum_{\rho,\tau} F_{\rho\tau}(\mathbf{R}_p)Q_p^{r,\rho}Q_p^{t,\tau}+\sum_p\sum_{\rho,\tau}\sum_{p'\neq p}\sum_{\rho',\tau'} Q_p^{r,\rho}Q_p^{t,\tau}X_{\rho\tau;\rho'\tau'}(\mathbf{R}_{pp'})Q_{p'}^{r,\rho'}Q_{p'}^{t,\tau'} . \quad (8)$$

The kinetic energy T_p^k is either translational, $T_p^t=T(\mathbf{u}_p)$, or rotational, $T_p^r=L(\omega_p)$, and the coefficients $F_{\rho\tau}(\mathbf{R}_p)$ and $X_{\rho\tau;\rho'\tau'}(\mathbf{R}_{pp'})$ are the same as in Eqs. (5) and (3). The complete expressions for these coefficients can be found in Ref. 45 and in Appendix A, respectively.

B. The time-dependent Hartree method

The first step in our treatment is a mean-field (MF) calculation. The translational and rotational motions are decoupled at this level so that we obtain two effective particles per molecule.[37] This yields the following MF Hamiltonian:

$$H_p^k=T_p^k+\sum_\nu c_p^{k,\nu}Q_p^{k,\nu} , \quad (9)$$

with

$$c_p^{k,\nu}=\sum_{\bar{\nu}}\langle Q_p^{\bar{k},\bar{\nu}}\rangle\left[F_{\nu\bar{\nu}}(\mathbf{R}_p)+\sum_{p'\neq p}\sum_{\rho',\tau'} X_{\nu\bar{\nu};\rho'\tau'}(\mathbf{R}_{pp'})\langle Q_p^{r,\rho'}\rangle\langle Q_p^{t,\tau'}\rangle\right] , \quad (10)$$

where $\bar{k}$ denotes the complement of the type of the motion k, i.e., $\bar{r}=t$ and $\bar{t}=r$. The thermodynamic average of a dynamical variable is defined by

$$\langle Q_p^{k,\nu}\rangle=\mathrm{Tr}^{(pk)}(d_p^k Q_p^{k,\nu}) , \quad (11)$$

i.e., by a single-particle trace with the MF density operator d_p^k. The MF equations

$$H_p^k|\psi_p^{k,a}\rangle=\varepsilon_p^{k,a}|\psi_p^{k,a}\rangle \quad (12)$$

are solved self-consistently in a basis of tesseral harmon-

ics (real spherical harmonics) for the rotational states ($k=r$) and three-dimensional harmonic oscillator functions for the translational vibrations ($k=t$). For the case at hand, we have included tesseral harmonics up to $l_{\max}=12$ or 13, for *ortho-* or *para*-N_2, respectively, and spherical harmonic oscillator functions up to principal quantum number $n_{\max}=6$.

The coupling between the molecular motions, neglected at the MF level, is regained with the aid of the time-dependent Hartree method. This method is briefly summarized in Appendix B. The excitation and deexcitation energies of the adsorbed layer that correspond with the translational phonons, the librons or, in general, with mixed modes of wave vector $\mathbf{q}$, are the eigenvalues of the following dynamical matrix:

$$\underline{M}(\mathbf{q})=\underline{\varepsilon}-\underline{P}\,\underline{Q}\,\underline{W}(\mathbf{q})\tilde{\underline{Q}}^{T} . \tag{13}$$

This matrix comprises the MF excitation energy matrix $\underline{\varepsilon}$ and the density operator difference matrix $\underline{P}$ with the elements

$$\varepsilon_{ikab;i'k'a'b'}=\delta_{ii'}\delta_{kk'}\delta_{aa'}\delta_{bb'}(\varepsilon_p^{k,a}-\varepsilon_p^{k,b}) \tag{14}$$

and

$$P_{ikab;i'k'a'b'}=\delta_{ii'}\delta_{kk'}\delta_{aa'}\delta_{bb'}(d_p^{k,a}-d_p^{k,b}) . \tag{15}$$

The molecules are labeled here by $p=\{\mathbf{n},i\}$, where $\mathbf{n}$ labels the unit cells and i the sublattices. Furthermore, Eq. (13) contains transition matrix elements

$$\begin{aligned} Q_{ikab;i'k'\nu}&=\delta_{ii'}\delta_{kk'}\langle\psi_p^{k,a}|Q_p^{k,\nu}|\psi_p^{k,b}\rangle , \\ \tilde{Q}_{ikab;i'k'\nu}&=Q_{ikba;i'k'\nu} , \end{aligned} \tag{16}$$

of the dynamical variables. The coupling information is contained in the Fourier transforms

$$W_{ik\nu;i'k'\nu'}(\mathbf{q})=\sum_{\mathbf{n}}\exp[i\mathbf{q}\cdot(\mathbf{R}_{p'}-\mathbf{R}_p)]W_{pp'}^{k\nu;k'\nu'} , \tag{17}$$

with $p=\{\mathbf{0},i\}$, $p'=\{\mathbf{n},i'\}$ and

$$W_{pp'}^{k\nu;k'\nu'}=(1-\delta_{pp'})\sum_{\bar{\nu}}\sum_{\bar{\nu}'}\langle Q_p^{\bar{k},\bar{\nu}}\rangle X_{\nu\bar{\nu};\nu'\bar{\nu}'}(\mathbf{R}_{pp'})\langle Q_{p'}^{\bar{k}',\bar{\nu}'}\rangle+\delta_{pp'}\delta_{k\bar{k}'}\left[F_{\nu\nu'}(\mathbf{R}_p)+\sum_{p''\neq p}\sum_{\rho,\tau}X_{\nu\nu';\rho\tau}(\mathbf{R}_{pp''})\langle Q_{p''}^{r,\rho}\rangle\langle Q_{p''}^{t,\tau}\rangle\right] . \tag{18}$$

The first term in Eq. (18) couples the motions of the molecules at different lattice sites; the other terms are translation-rotation couplings on the same site. Both the molecule-substrate potential and the intermolecular potential are active in the latter.

It is proved in Appendix B that the TDH method is exactly equivalent to the approach that uses generalized susceptibilities.[42–44] The frequency-dependent single-particle susceptibility corresponds with the MF model and it is given in terms of the matrices in Eqs. (13), (14), and (15) by

$$\underline{\chi}^{(0)}(\omega)=\tilde{\underline{Q}}^{T}(\omega-\underline{\varepsilon})^{-1}\underline{P}\,\underline{Q} . \tag{19}$$

The generalized crystal susceptibility $\underline{\chi}(\mathbf{q},\omega)$ for wave vector $\mathbf{q}$ is related[42] to $\underline{\chi}^{(0)}(\omega)$ and to the coupling matrix $\underline{W}(\mathbf{q})$ in Eq. (17) by the Dyson equation

$$\underline{\chi}(\mathbf{q},\omega)^{-1}=\underline{\chi}^{(0)}(\omega)^{-1}+\underline{W}(\mathbf{q}) . \tag{20}$$

It is shown in Appendix B that the frequencies of the poles in $\underline{\chi}(\mathbf{q},\omega)$ are exactly equal to the eigenvalues of the dynamical matrix $\underline{M}(\mathbf{q})$ in Eq. (13), i.e., to the (de)excitation frequencies of the crystal calculated by the TDH method.

Before we present the results we mention some further computational details. The width parameter A in the three-dimensional harmonic-oscillator basis[37] for the center-of-mass vibrations is chosen as $A=(m\omega/\hbar)^{1/2}$, where m is the nitrogen molecular mass and ω is the average of the MF fundamental excitation frequencies. We use 1.42 Å as the nearest-neighbor distance between the carbon atoms within the graphite layers and 3.37 Å as the distance between the layers. If not indicated otherwise, we have used Steele's[40] parameters $\sigma=3.343$ Å and $\varepsilon=0.2631$ kJ/mol in the atom-atom model for the molecule-substrate potential. Only the top layer of the graphite substrate contributes to the corrugation (i.e., the terms with $\mathbf{g}\neq\mathbf{0}$) in this potential. It is summed over molecule-atom pairs within a range of 30 Å. The next ten underlying graphite layers are taken into account in the first Fourier term ($\mathbf{g}=\mathbf{0}$) in Eq. (6) by analytic summation.[45] The intermolecular potential in the adsorbed layer is summed over 8.1 Å and the rotational constant of N_2 is taken as $B=2.013$ cm^{-1}. All calculations are performed at zero temperature.

III. RESULTS AND DISCUSSION

In order to illustrate the effects of the anharmonicity and the corrugation in the potential we compare the results of the full TDH calculations with more approximate treatments. The first approximation consists of limiting the dynamical variables, see Eq. (7), to the terms with $\alpha_1+\alpha_2\leq\alpha_{\max}=2$. This approximation implies that the Hamiltonian in Eq. (8) becomes harmonic in the translational displacements. The anharmonicity in the librations is fully retained through the expansion in spherical harmonics. The next level of approximation is a pure harmonic treatment based on the spherical expansion (SE) of the *ab initio* intermolecular potential,[33] cf. Eq. (2). The required first and second derivatives of this potential with respect to the translational and librational displacements are given in Ref. 39. Finally, we compare also some results obtained with the site-site (SS) model potential[33] that was fitted to the *ab initio* data. In order to study the effects of the surface corrugation we may switch off this corrugation at the various levels, as has been done previously in (quasi)harmonic calculations.[21,23]

We will not distinguish between *ortho*- and *para*-N_2 layers, since the MF and TDH calculations with even or odd l free-rotor functions in the basis yield practically the same results for the ordered phases considered here.

A. Commensurate monolayers

First we discuss the results for the commensurate $(\sqrt{3}\times\sqrt{3})R30°$ monolayer with the nearest-neighbor distance of 4.26 Å fixed by the substrate. It is illustrative to begin with the fundamental excitations at the single-particle level (see Table I). Even in the fully anharmonic TDH treatment it is easy to recognize the normal mode contents of the translational vibrations and librations and to assign the corresponding quantum numbers. Especially for the librations this is striking since their wave functions have been expanded in a free-rotor basis. The frequencies of overtones and combination bands are surprisingly close to the sums of the fundamental frequencies. Also the adsorption energy is close to the harmonic value including the zero-point motions.

Still, one clearly observes the frequency shifts which are due to the anharmonicity. For the out-of-plane translational motions there is already a difference between the harmonic calculations and the MF calculations with $\alpha_{max}=2$. This may be unexpected since these calculations use exactly the same potential and the MF scheme with $\alpha_{max}=2$ involves a Hamiltonian that is harmonic in the center-of-mass displacements. We have found that the difference is due to the averaging over (anharmonic) librations which is performed in the MF calculations with $\alpha_{max}=2$, but not in the harmonic treatment. When the cubic and quartic ($\alpha=3$ and 4) displacement terms are switched on, we find an upward shift of about 4.5 cm^{-1} for the in-plane vibrations and a downward shift of 5.4 cm^{-1} for the out-of-plane vibration. In order to understand this result we remind the reader that the commensurate adsorbed layer cannot expand in the parallel directions, but it can be lifted from the surface by the anharmonicity. It has been observed already[45] that the potential is strongly anharmonic in the z direction and we find here that the average center-of-mass positions are higher by $\langle u_z\rangle=\langle z\rangle-z_e=0.054$ Å than the static equilibrium positions. For the librations we find anharmonic shifts of about -3.2 cm^{-1} and a further shift of -4.1 cm^{-1} in the out-of-plane libration when the anharmonic displacement terms are switched on. The latter shift is caused by the lifting of the adsorbed layer.

In Figs. 1 and 2 we show the phonon and libron dispersion curves calculated by the TDH method. These curves are similar to the harmonic results.[21] Due to an artificial symmetry which is present only at the harmonic level one can decouple[21] the in-plane motions from the out-of-plane motions by switching off the corrugation in

TABLE I. Single-particle excitations in the $(\sqrt{3}\times\sqrt{3})R30°$ monolayer.

	Mean field		Harmonic		Mode
	$\alpha_{max}=4$	$\alpha_{max}=2$	self-term		character[a]
ω_T (cm^{-1})	34.7	30.4	29.7	1 0 0	(in-plane)
	42.0	37.3	36.7	0 1 0	
	55.7	61.1	57.7	0 0 1	(out-of-plane)
	71.3	61.5	59.4	2 0 0	
	77.4	68.0	66.4	1 1 0	(overtones
	86.0	74.7	73.4	0 2 0	and
	90.4	92.0	87.4	1 0 1	combinations)
	96.7	98.7	94.4	0 1 1	
ω_L (cm^{-1})	48.0	52.1	55.3	1 0	(out-of-plane ϑ)
	52.4	52.8	55.9	0 1	(in-plane φ)
	96.6	102.3	110.6	2 0	(overtones
	99.0	103.7	111.2	1 1	and
	104.8	108.2	111.8	0 2	combinations)
z_e (Å)	3.305	3.305	3.305		
$\langle u_z\rangle$ (Å)	0.054	0.025			
$\langle u_x^2\rangle^{1/2}$ (Å)	0.124	0.132			
$\langle u_y^2\rangle^{1/2}$ (Å)	0.128	0.136			
$\langle u_z^2\rangle^{1/2}$ (Å)	0.117	0.103			
φ_e (deg)	42[b]	42[b]	42.0		
$\langle\cos^2\vartheta\rangle$	0.040	0.037			
$\langle\sin^2\vartheta\cos2\varphi\rangle$	0.059	0.060			
$\langle\sin^2\vartheta\sin2\varphi\rangle$	0.884	0.887			
E (kJ/mol)	−11.143	−11.145	−11.130/−12.537[c]		

[a]Three vibrational quantum numbers are assigned to the translations and two to the librations.
[b]These numbers indicate the maximum in orientational probability.
[c]Including or without the zero-point vibrations.

the molecule-substrate potential. At the TDH level only the natural symmetry of the system occurs and we study the effect of the in-plane and out-of-plane (de)coupling by the omission of the corresponding coupling terms in the TDH matrix given by Eq. (13). Even in the decoupled curves in Fig. 1 we have retained the $\mathbf{g}\neq\mathbf{0}$ contributions in the molecule-substrate potential, as evident by the presence of the phonon gap. Comparison of Figs. 1 and 2 shows that also in the full TDH computations there is a near separation between the in-plane and out-of-plane motions. This separation and also the observed near separation between the translational phonons and the librons holds in the entire Brillouin zone, except near the avoided crossings. The in-plane motions are primarily determined by the N_2-N_2 intralayer potential, the out-of-plane motions by the N_2-substrate potential. Yet, we observe in Figs. 1 and 2 that the dispersion of the out-of-plane libron frequencies is substantial. The out-of-plane translational phonon band is very flat indeed.

The $\mathbf{q}=\mathbf{0}$ phonon and libron frequencies, as computed at the different levels of approximation, are given in Table II. The lowest two values are the frequencies of the acoustic-phonon modes which are not equal to zero because of the corrugation in the molecule-substrate potential. These values characterize the so-called phonon gap.[13–15] The translational and librational anharmonicities appear to have very little influence on this gap. The anharmonic shifts in the optical-phonon frequencies and in the libron frequencies are strikingly similar to the shifts discussed at the single-particle level. So, these shifts are mainly determined by the anharmonicity in the field experienced by an adsorbed molecule, which is due to the other molecules in the layer as well as to the sub-

TABLE II. Lattice frequencies for $\mathbf{q}=\mathbf{0}$ (in cm^{-1}) for the commensurate $(\sqrt{3}\times\sqrt{3})R30°$ monolayer.

Symmetry group $p2gg$		TDH $\alpha_{max}=4$	TDH $\alpha_{max}=2$	Harmonic SE[a]	Harmonic SS[b]
In-plane translations	B_1	6.9	7.4	6.2	6.4
	B_2	7.1	7.7	6.8	6.6
	B_2	35.6	33.0	32.7	35.9
	B_1	48.8	43.2	42.7	43.9
Out-of-plane librations	B_2	40.6	44.7	47.6	47.5
	B_1	51.6	54.1	57.1	57.2
Out-of-plane translations	A_1	55.9	60.6	57.4	57.4
	A_2	55.5	61.1	57.7	57.7
In-plane librations	A_1	60.4	61.2	63.3	59.7
	A_2	69.9	70.5	75.0	68.9

[a]Using the same spherically expanded *ab initio* N_2-N_2 potential as in TDH; equilibrium height $z_e=3.305$ Å, angle $\varphi_e=42.0°$, and static absorption energy $E=-12.537$ kJ/mol.
[b]Using the site-site model (Ref. 33) for the *ab initio* N_2-N_2 potential; equilibrium height $z_e=3.305$ Å, angle $\varphi_e=44.0°$, and static adsorption energy $E=-12.618$ kJ/mol.

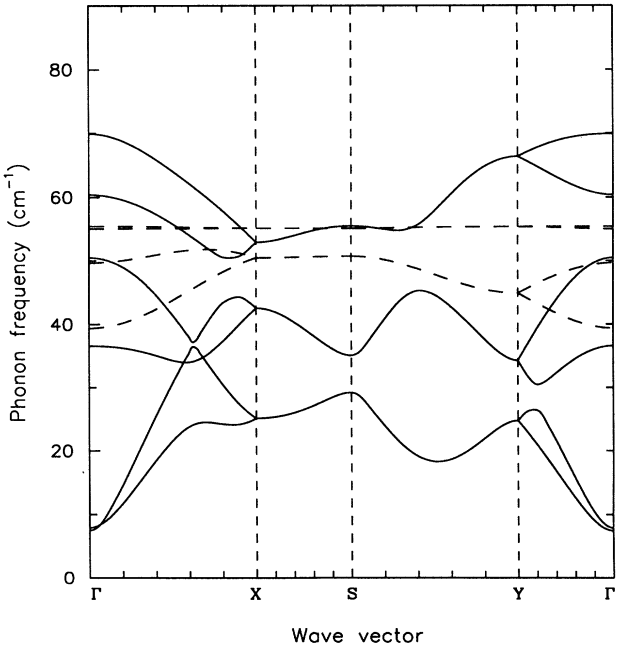

FIG. 1. Phonon-libron dispersion curves for a commensurate $(\sqrt{3}\times\sqrt{3})R30°$ N_2 monolayer on graphite from TDH calculations ($\alpha_{max}=4$). In-plane (solid curves) and out-of-plane (dashed curves) branches have been decoupled by the omission of coupling blocks in the TDH matrix of Eq. (13).

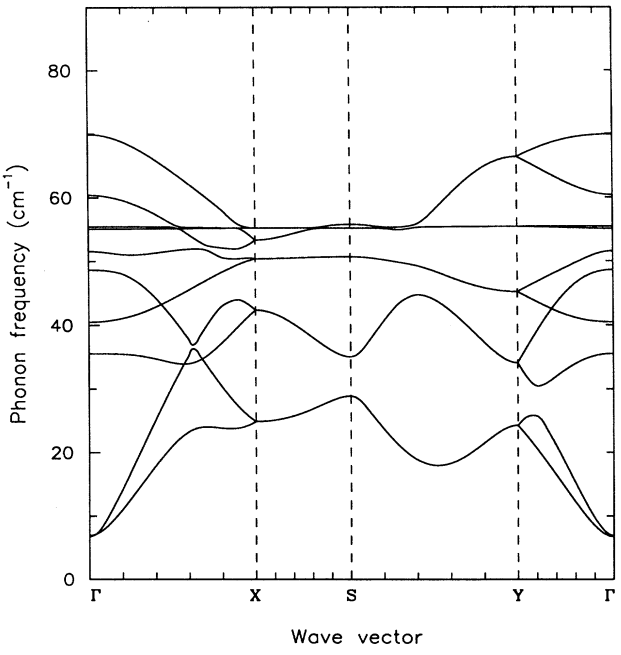

FIG. 2. Phonon-libron dispersion curves for a commensurate $(\sqrt{3}\times\sqrt{3})R30°$ N_2 monolayer on graphite from TDH calculations ($\alpha_{max}=4$). Symmetry group $p2gg$, Brillouin zone points $\Gamma=(0,0)$, $X=(\pi/a,0)$, $Y=(0,\pi/b)$, and $S=(\pi/a,\pi,b)$.

strate atoms. The difference between the site-site model of the N_2-N_2 potential and its representation by the spherical expansion is mostly apparent in the frequencies of the in-plane phonons and librons, as might be expected. The effect on the libron frequencies is substantially smaller than in bulk nitrogen, however.[39]

Next we compare our results with the data obtained from inelastic neutron scattering.[13–15] The quantities that have been measured are a phonon gap of 13.4 cm^{-1}, the frequency of the out-of-plane translational phonons ≈ 50 cm^{-1}, the width of the in-plane phonon and libron density of states ≈ 45 cm^{-1}, and the average frequency of this density of states ≈ 36 cm^{-1}. The latter two quantities are rather global and they are consistent with the calculations. For the frequency of the out-of-plane phonon band we find a value of 56 cm^{-1}. The corresponding harmonic value is 58 cm^{-1}, both in our calculations and in Ref. 21. The calculated phonon gap of 6.9 cm^{-1} is too small by a factor of 2, as in the previous harmonic calculations.[15,21]

Since the largest uncertainty in the calculations concerns the molecule-substrate potential we have systematically varied the Lennard-Jones parameters σ and ε in the atom-atom model for this potential. The results, which are listed in Table III, can be summarized as follows. As expected, the frequencies of the in-plane optical phonons and librons are rather insensitive to the parameters in the N_2-substrate potential. The out-of-plane frequencies depend only slightly on the parameter σ, although the height of the adsorbed layer and the adsorption energy change considerably with σ. The dependence of the out-of-plane frequencies on the well-depth parameter ε is nearly as $\varepsilon^{1/2}$. The acoustic-phonon gap depends on σ and ε, but it does not reach a value that is close to the experimental number. So we must conclude that an atom-atom model as used here and in other calculations[15,19–31] for the molecule-substrate potential cannot represent the correct surface corrugation. This holds even when the parameters in this model are varied, within limits that are reasonable in view of the measured adsorption energy[51] and the out-of-plane phonon frequency of ≈ 50 cm^{-1}.

B. Incommensurate monolayers

The results for the incommensurate monolayers have been calculated by switching off the corrugation, i.e., omitting the $\mathbf{g} \neq \mathbf{0}$ contributions, in the molecule-substrate potential. First we have optimized the structure, i.e., the two-dimensional lattice parameters and the height of the adsorbed molecules above the substrate. For the herringbone structure with $p2gg$ symmetry the lattice parameters a and b have been varied independently; there are two molecules in the unit cell with the same height, which may lie (on the average) within the layer plane or they may be tilted out of the plane. For the pinwheel structure[23] with $p6$ symmetry there is only one independent lattice parameter and there are four molecules in the unit cell. The height of the pin molecule above the substrate will be different from the height of the three wheel molecules, so these heights have been optimized independently. The wheel molecules may be tilted out of the layer plane.

Minimization of the static energy for the herringbone structure at zero pressure yields $a=4.224$ Å, $b=7.124$ Å and the energy $E=-12.486$ kJ/mol. The MF calculations yield $a=4.36$ Å and $b=7.21$ Å with energy $E=-11.036$ kJ/mol, so it is essential to include the zero-point motions. The latter value of a is even larger than the corresponding lattice parameter for the commensurate monolayer, but we note here that the incom-

TABLE III. Lattice frequencies (in cm^{-1}) for the $(\sqrt{3}\times\sqrt{3})R30°$ monolayer as a function of the molecule-substrate interaction parameters σ and ε (from harmonic calculations with the spherical expansion of the N_2-N_2 potential).

	ε (kJ/mol)	0.20	0.20	0.20	0.20	0.25	0.25	0.25	0.25	0.30	0.30	0.30	0.30
	σ (Å)	2.5	3.0	3.5	4.0	2.5	3.0	3.5	4.0	2.5	3.0	3.5	4.0
Height	z_e (Å)	2.436	2.957	3.463	3.958	2.436	2.957	3.463	3.958	2.436	2.957	3.463	3.958
Angle	φ_e (deg)	41.96	41.98	41.99	41.99	41.95	41.98	41.99	41.99	41.94	41.98	41.99	41.99
Static energy	E (kJ/mol)	−6.88	−8.68	−11.00	−13.89	−7.87	−10.15	−13.04	−16.66	−8.91	−11.61	−15.09	−19.43
In-plane translations	B_1	5.1	6.1	5.1	3.8	5.5	6.7	5.7	4.2	5.9	7.4	6.2	4.6
	B_2	1.4	6.2	5.5	4.5	4.3	7.2	6.2	4.7	5.5	8.1	6.8	5.1
	B_2	29.9	31.6	32.4	32.4	31.3	32.4	32.6	32.5	32.0	32.7	32.8	32.6
	B_1	41.5	42.4	42.5	42.5	42.2	42.7	42.6	42.4	42.7	42.9	42.7	42.5
Out-of-plane librations	B_2	40.8	38.9	39.0	40.2	46.8	45.5	46.2	47.6	52.5	51.6	52.5	54.0
	B_1	50.6	49.7	50.2	51.2	55.8	55.3	56.0	57.2	60.8	60.4	61.3	62.6
Out-of-plane translations	A_1	49.2	49.6	50.3	51.2	55.0	55.5	56.3	57.2	60.3	60.7	61.6	62.7
	A_2	49.6	50.0	50.6	51.5	55.3	55.7	56.5	57.5	60.6	61.0	61.9	63.0
In-plane librations	A_1	63.4	63.3	63.3	63.3	63.4	63.3	63.3	63.3	63.5	63.3	63.3	63.3
	A_2	75.1	75.0	75.0	75.0	75.1	75.1	75.0	75.0	75.1	75.1	75.0	75.0

mensurate phases are stable only at higher pressure. For the pinwheel structure the MF calculations yield nearest-neighbor distance $a=4.14$ Å and $E=-10.895$ kJ/mol with average heights $\langle z \rangle = 3.382$ and 3.742 Å for the wheel and pin molecules, respectively. The wheel molecules lie within the layer with $\varphi=40°$, 160°, and 280° and the pin molecules are indeed localized around the z direction. The amplitude in the angle ϑ is substantially larger for the pin molecules (23°) than it is for the wheel molecules (11°) and the fundamental librational frequency is considerably smaller (33.0 cm^{-1}, twofold degenerate, versus 49.7 cm^{-1}, out-of-plane, and 52.3 cm^{-1}, in-plane). All these results for the wheel molecules are similar to the corresponding values for the molecules in the herringbone layer shown in Table I, but the pin molecules behave rather differently.

In order to perform the calculations for non-zero two-dimensional pressures we proceed as follows. For the herringbone structure we choose a grid of three points a and three points b around the values of the lattice parameters which we expect to find for a given pressure. We calculate the MF energies at these grid points and we fit these energies by a second-order form in a and b. From this form it is easy to determine the ratio b/a that minimizes the MF energy for constant surface $s=\frac{1}{2}ab$. At zero temperature the MF energy is equal to the Helmholtz free energy A. On the curve of optimized b/a ratios we calculate the two-dimensional pressure $p=-(\partial A/\partial s)_T$, as well as the chemical potential $\mu=A+ps$. This procedure has been repeated for different grids, i.e., different ranges of s and p, in order to obtain the $\mu(s)$, $\mu(p)$, and $p(s)$ curves for the herringbone structure. The corresponding procedure for the pinwheel structure is trivial, since there is only one independent lattice parameter. Only the optimization of the heights of the pin and the wheel molecules is tedious.

The molecules in the herringbone layer stay within the plane and the optimized b/a ratio is equal to about 1.65 for the whole range of pressures investigated ($p \leq 0.090$ N/m which corresponds to $a \geq 4.15$ Å). For still higher pressures corresponding with $a=4.05$ Å and $b=6.68$ Å the herringbone structure becomes unstable; one of the TDH frequencies is imaginary. The ratio $b/a=1.65$ implies a reduction of 5% with respect to the value of $\sqrt{3}$ that holds for the commensurate monolayer, in good agreement with the experimental observation[52] that the monolayer structure for a range of pressures is uniaxially incommensurate with a reduction in b that ranges from 2 to 5%. For the pinwheel structure the wheel molecules stay within the layer also. The calculated $\mu(p)$ curves for the herringbone and pinwheel structures are similar to those in Ref. 23. At zero pressure we find with the use of the *ab initio* N_2-N_2 potential that the herringbone structure is more stable than the pinwheel structure by 0.14 kJ/mol. The pinwheel structure is considerably more compact, however, so it will be favored at higher pressures. Since the $\mu(p)$ curves run nearly parallel it is hard to determine the transition pressure. From the difference in surface per molecule, $s=15.76$ $Å^2$ for the herringbone layer and $s=14.84$ $Å^2$ for the pinwheel layer, we estimate that the transition occurs around $p=0.025$ N/m. The chemical potential $\mu=-8.62$ kJ/mol at this pressure is considerably lower than the bulk value of -5.92 kJ/mol (Ref. 37) and it is lower also than the value of -7.3 kJ/mol estimated[23] for the beginning of bilayer formation. So we conclude that the incommensurate monolayer may adopt the pinwheel ordering at higher pressures.

The phonon and libron dispersion curves for the optimized incommensurate herringbone layer with $a=4.15$ Å, $b=6.87$ Å, and $s=14.25$ Å are shown in Fig. 3 and the optical ($\mathbf{q}=\mathbf{0}$) frequencies are listed in Table IV. Although some of the avoided crossings occur at different points in the Brillouin zone, Fig. 3 is qualitatively not so different from Fig. 2. The frequencies of the in-plane modes are considerably higher, however, and their dispersion is larger, due to the compression of the adsorbed layer. Note that there is no phonon gap for $\mathbf{q}=\mathbf{0}$, of course, since there is no corrugation in the molecule-substrate potential. The anharmonic frequency shifts are similar to those discussed for the commensurate monolayer, but slightly larger. Especially the large downward shift of the lowest out-of-plane libration is noticeable. The low frequency of this libration and its large anharmonicity are the signs of this mode becoming soft and the molecules wanting to rotate out of the plane at still higher pressures. The phonon and libron curves for the pinwheel structure are drawn in Fig. 4 and the character

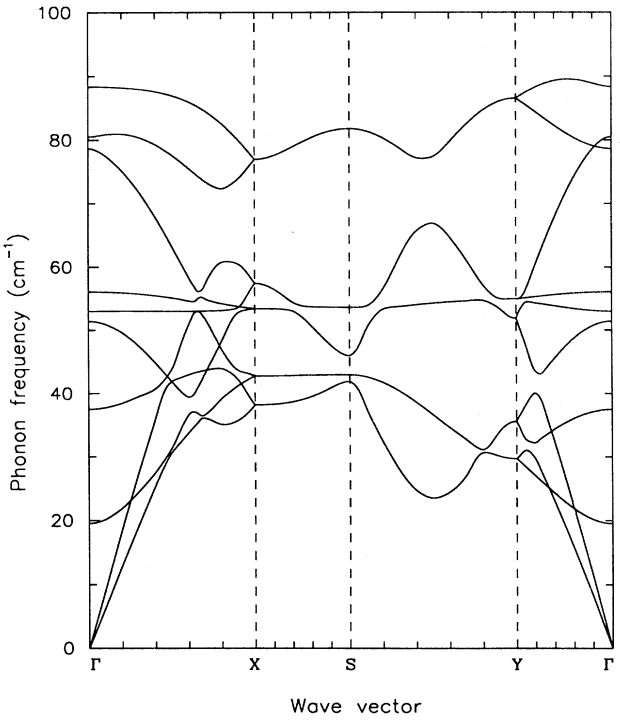

FIG. 3. Phonon-libron dispersion curves for an incommensurate N_2 herringbone monolayer on graphite from TDH calculations ($\alpha_{max}=4$) with the uncorrugated ($\mathbf{g}=\mathbf{0}$) molecule-substrate potential. Lattice constants $a=4.15$ Å, $b=6.87$ Å.

TABLE IV. Lattice frequencies for $\mathbf{q}=\mathbf{0}$ for the incommensurate herringbone monolayer (lattice constants $a=4.15$ Å and $b=6.87$ Å).

Symmetry group $p2gg$		TDH $\alpha_{max}=4$	TDH $\alpha_{max}=2$	Harmonic SE[a]	Harmonic SS[a]
Height	z_e (Å)	3.324	3.324	3.324	3.324
	$\langle u_z \rangle$ (Å)	0.064	0.031		
Angle	φ_e (deg)	40	40	38.9	40.3
Energy	E (kJ/mol)	−10.716	−10.705	−12.380[b]	−12.393[b]
		Lattice frequencies (cm^{-1})			
In-plane translations	B_1	0.0	0.0	0.0	0.0
	B_2	0.0	0.0	0.0	0.0
	B_2	51.4	48.7	49.2	55.1
	B_1	80.5	74.8	76.3	78.9
Out-of-plane librations	B_2	19.5	27.3	25.2	30.3
	B_1	37.5	42.7	44.2	46.9
Out-of-plane translations	A_2	53.0	60.0	55.0	54.9
	A_1	56.1	62.1	57.5	57.6
In-plane librations	A_1	78.6	79.6	84.5	79.6
	A_2	88.4	89.9	96.2	88.7

[a]With different N_2-N_2 potentials, as in Table II.
[b]Not including zero-point motions.

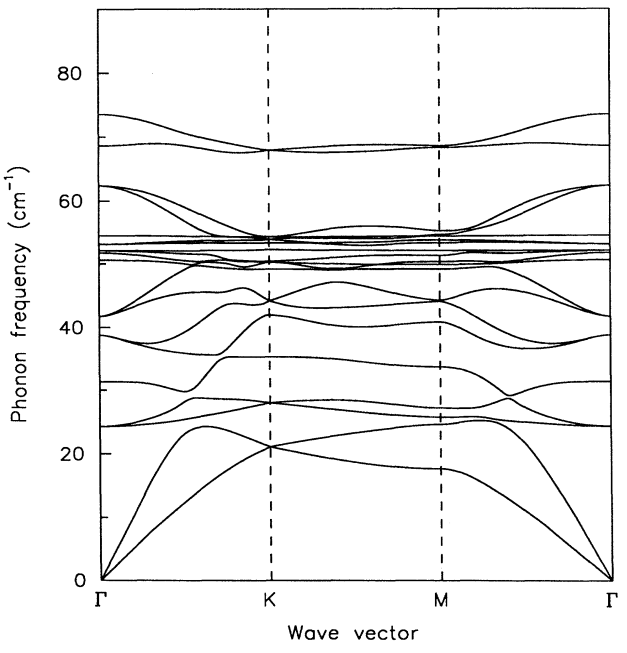

FIG. 4. Phonon-libron dispersion curves for an incommensurate N_2 pinwheel monolayer on graphite from TDH calculations ($\alpha_{max}=4$) with the uncorrugated ($\mathbf{g}=\mathbf{0}$) molecule-substrate potential. Nearest-neighbor distance $a=4.057$ Å. Symmetry group $p6$, Brillouin zone points $\Gamma=(0,0)$, $K=(2\pi/3a,0)$, and $M=(\pi/2a,\pi/2a\sqrt{3})$.

of the modes for $\mathbf{q}=\mathbf{0}$ is indicated in Table V. Due to the different symmetry and the fact that this structure contains two distinct types of molecules the resulting picture is rather different from the dispersion curves for the herringbone layer. We observe also that the frequencies are much lower, although the calculations leading to Figs. 3 and 4 have been performed for the same surface per mol-

TABLE V. Lattice frequencies for $\mathbf{q}=\mathbf{0}$ (in cm^{-1}) for the incommensurate pinwheel monolayer (nearest-neighbor distance $a=4.075$ Å).

Symmetry group $p6$		TDH $\alpha_{max}=4$	
In-plane translations	E_1	0.0	pin+wheel
	B	31.4	wheel
	E_1	38.8	pin+wheel
	E_1	62.4	pin+wheel
	B	73.5	wheel
Out-of-plane librations	E_1	24.3	pin+wheel
	B	50.6	wheel
	E_1	52.1	pin+wheel
Out-of-plane translations	A	51.7	pin
	E_2	53.1	wheel
	A	54.5	pin+wheel
In-plane librations	E_2	41.7	wheel
	A	68.8	wheel

ecule ($s=14.25$ Å^2). This is related to the pressure which is substantially lower for the pinwheel ordering than for the herringbone structure. To our knowledge the phonon frequencies for the incommensurate monolayers have not been measured yet.

ACKNOWLEDGMENTS

We thank Wilfred Janssen, Thijs Bongers, and Henri de Bekker for their assistance with the calculations. The investigations were supported in part by the Netherlands Foundation for Chemical Research (SON) with financial aid from the Netherlands Organization for Scientific Research (NWO). Part of this work has been performed as an IBM Academic Information Systems (ACIS) project.

APPENDIX A

In Ref. 37 the intermolecular potential given by Eq. (2) is written as a double Taylor expansion in the center-of-mass displacements $\mathbf{u}_p$ and $\mathbf{u}_{p'}$. Here, we derive a similar expansion in a form that is amenable to much faster numerical calculation. First we expand the part of the potential that depends on the displacements as a Taylor series in $\mathbf{u}_{pp'}=\mathbf{u}_{p'}-\mathbf{u}_p$

$$\varphi_l(r_{pp'})C_{m_3}^{(l_3)}(\hat{\mathbf{r}}_{pp'})=\sum_{\alpha=0}^{\infty}\frac{(\mathbf{u}_{pp'}\cdot\nabla)^\alpha}{\alpha!}\varphi_l(R_{pp'})C_{m_3}^{(l_3)}(\hat{\mathbf{R}}_{pp'}) . \tag{A1}$$

We can evaluate this expression by means of the gradient formula in spherical tensor form[53]

$$\mathbf{u}_{pp'}\cdot\nabla\varphi_l(R_{pp'})C_{m_3}^{(l_3)}(\hat{\mathbf{R}}_{pp'})=u_{pp'}\sum_{k_1}A_{l_3k_1}(R_{pp'})\varphi_l(R_{pp'})(-1)^{m_3}\sum_{n_1,n_2}\begin{bmatrix}1 & k_1 & l_3\\ n_1 & n_2 & -m_3\end{bmatrix}C_{n_1}^{(1)}(\hat{\mathbf{u}}_{pp'})C_{n_2}^{(k_1)}(\hat{\mathbf{R}}_{pp'}) , \tag{A2}$$

where the operator $A_{l_3k_1}(R_{pp'})$ is given by

$$A_{l_3k_1}(R_{pp'})=(-1)^{l_3}\left[\delta_{k_1,l_3-1}\left[\frac{l_3(2l_3-1)}{2l_3+1}\right]^{1/2}\left[\frac{d}{dR_{pp'}}+\frac{l_3+1}{R_{pp'}}\right]-\delta_{k_1,l_3+1}\left[\frac{(l_3+1)(2l_3+3)}{2l_3+1}\right]^{1/2}\left[\frac{d}{dR_{pp'}}-\frac{l_3}{R_{pp'}}\right]\right] . \tag{A3}$$

The use of this relation in Eq. (A1) gives

$$\varphi_l(r_{pp'})C_{m_3}^{(l_3)}(\hat{\mathbf{r}}_{pp'})=\sum_{\alpha}\frac{(u_{pp'})^\alpha}{\alpha!}\sum_{k_1,k_2}{}^lW_{k_1k_2}^{(\alpha)}(R_{pp'})\sum_{n_1,n_2}(-1)^{m_3}\begin{bmatrix}k_1 & k_2 & l_3\\ n_1 & n_2 & -m_3\end{bmatrix}C_{n_1}^{(k_1)}(\hat{\mathbf{u}}_{pp'})C_{n_2}^{(k_2)}(\hat{\mathbf{R}}_{pp'}) . \tag{A4}$$

The coefficients ${}^lW_{k_1k_2}^{(\alpha)}(R_{pp'})$ can be calculated with the following recursion relation:

$${}^lW_{k_1k_2}^{(\alpha)}(R_{pp'})=(2k_1+1)(-1)^{l_3+1}\sum_{j_1,j_2}\begin{bmatrix}j_1 & 1 & k_1\\ 0 & 0 & 0\end{bmatrix}\begin{Bmatrix}k_2 & k_1 & l_3\\ j_1 & j_2 & 1\end{Bmatrix}A_{j_2k_2}(R_{pp'}){}^lW_{j_1j_2}^{(\alpha-1)}(R_{pp'}) , \tag{A5}$$

with

$${}^lW_{k_1k_2}^{(0)}(R_{pp'})=\delta_{k_1,0}\delta_{k_2,l_3}\sqrt{2l_3+1}\varphi_l(R_{pp'}) , \tag{A6}$$

while the expression in curly braces is a 6-j coefficient.

Now we can split $(u_{pp'})^\alpha C_{n_1}^{(k_1)}(\hat{\mathbf{u}}_{pp'})$ in factors dependent on the molecular displacements $\mathbf{u}_p$ and $\mathbf{u}_{p'}$ (Ref. 54)

$$(u_{pp'})^\alpha C_{n_1}^{(k_1)}(\hat{\mathbf{u}}_{pp'})=\sum_{\alpha_1=0}^{\alpha}\sum_{\lambda_1=0}^{\alpha_1}\sum_{\lambda_2=|k_1-\lambda_1|}^{\min(k_1+\lambda_1,\alpha_2)}\sum_{\mu_1}\sum_{\mu_2}B_{\alpha_1\lambda_1\mu_1\alpha_2\lambda_2\mu_2}^{\alpha k_1 n_1}(u_p)^{\alpha_1}C_{\mu_1}^{(\lambda_1)}(\hat{\mathbf{u}}_p)(u_{p'})^{\alpha_2}C_{\mu_2}^{(\lambda_2)}(\hat{\mathbf{u}}_{p'}) , \tag{A7}$$

where α_2 is given by $\alpha_2=\alpha-\alpha_1$ and the coefficients are

$$B_{\alpha_1\lambda_1\mu_1\alpha_2\lambda_2\mu_2}^{\alpha k_1 n_1}=(-1)^{\lambda_1+n_1}\frac{(\alpha+k_1+1)!!(\alpha-k_1)!!(2\lambda_1+1)(2\lambda_2+1)}{(\alpha_1+\lambda_1+1)!!(\alpha_1-\lambda_1)!!(\alpha_2+\lambda_2+1)!!(\alpha_2-\lambda_2)!!}\begin{bmatrix}k_1 & \lambda_1 & \lambda_2\\ 0 & 0 & 0\end{bmatrix}\begin{bmatrix}k_1 & \lambda_1 & \lambda_2\\ -n_1 & \mu_1 & \mu_2\end{bmatrix} . \tag{A8}$$

Introducing this into Eq. (2) and Eq. (A4), the intermolecular potential reads

$$\Phi_{pp'}(\mathbf{u}_p,\boldsymbol{\omega}_p,\mathbf{u}_{p'},\boldsymbol{\omega}_{p'})=\sum_{\Lambda_1}\sum_{\Lambda_2}(u_p)^{\alpha_1}C_{\mu_1}^{(\lambda_1)}(\hat{\mathbf{u}}_p)C_{m_1}^{(l_1)}(\boldsymbol{\omega}_p)X_{\Lambda_1\Lambda_2}(\mathbf{R}_{pp'})(u_{p'})^{\alpha_2}C_{\mu_2}^{(\lambda_2)}(\hat{\mathbf{u}}_{p'})C_{m_2}^{(l_2)}(\boldsymbol{\omega}_{p'}) , \tag{A9}$$

where Λ stands for the set of indices $\{\alpha,\lambda,\mu,l,m\}$ and $X_{\Lambda_1\Lambda_2}$ is given by

$$X_{\Lambda_1\Lambda_2}(\mathbf{R}_{pp'})=\sum_{l_3,m_3}\begin{bmatrix} l_1 & l_2 & l_3 \\ m_1 & m_2 & m_3 \end{bmatrix}\sum_{k_1,k_2}{}^{l}W_{k_1k_2}^{(\alpha_1+\alpha_2)}(R_{pp'})\sum_{n_1}\sum_{n_2}(-1)^{m_3}\begin{bmatrix} k_1 & k_2 & l_3 \\ n_1 & n_2 & -m_3 \end{bmatrix}C_{n_2}^{(k_2)}(\hat{\mathbf{R}}_{pp'})B^{\alpha_1+\alpha_2 k_1 n_1}_{\alpha_1\lambda_1\mu_1\alpha_2\lambda_2\mu_2}\ . \tag{A10}$$

This expansion is considerably simpler than that given in Ref. 37 because only one recurrence relation is needed for the coefficients ${}^{l}W_{k_1k_2}^{(\alpha)}(R_{pp'})$, instead of two.

APPENDIX B

The TDH method can be derived[37,41] by looking at the response of a system to a time-dependent perturbation. It is assumed that this perturbation can be represented by a sum of single-particle operators $h_p^k(t)$ and that the perturbed density operator is a product of single-particle density operators $d_p^k(t)=d_p^k+\delta_p^k(t)$. The density operators d_p^k correspond to the unperturbed MF model and the operators $\delta_p^k(t)$ describe the response of the system to the perturbation. The column vectors $\underline{h}(\mathbf{q},\omega)$ and $\underline{\delta}(\mathbf{q},\omega)$ contain the space-time Fourier transforms of the transition matrix elements of the single-particle operators $h_p^k(t)$ and $\delta_p^k(t)$ in a (finite) basis of MF states $\psi_p^{k,a}$

$$h_{ikab}(\mathbf{q},\omega)=(2\pi N)^{-1/2}\int dt\,\exp(i\omega t)\times\sum_{\mathbf{n}}\exp(i\mathbf{q}\cdot\mathbf{R}_p)\langle\psi_p^{k,a}|h_p^k(t)|\psi_p^{k,b}\rangle \tag{B1}$$

and

$$\delta_{ikab}(\mathbf{q},\omega)=(2\pi N)^{-1/2}\int dt\,\exp(i\omega t)\times\sum_{\mathbf{n}}\exp(i\mathbf{q}\cdot\mathbf{R}_p)\langle\psi_p^{k,a}|\delta_p^k(t)|\psi_p^{k,b}\rangle\ . \tag{B2}$$

As shown in Ref. 37 the Liouville equation, which describes the time evolution of the density operator, reduces in first order to the linear response equation

$$[\omega-\underline{M}(\mathbf{q})]\underline{\delta}(\mathbf{q},\omega)=-\underline{P}\,\underline{h}(\mathbf{q},\omega)\ . \tag{B3}$$

The density operator difference matrix $\underline{P}$ is given by Eq. (15) and the matrix $\underline{M}(\mathbf{q})$ by Eq. (13). The TDH (de)excitation energies are the eigenvalues of the matrix $\underline{M}(\mathbf{q})$.

The response properties of the system as given by Eq. (B3) can also be expressed by the generalized susceptibility $\underline{\chi}(\mathbf{q},\omega)$. To that end, we define the perturbation $h_p^k(t)$ as the action of an external field with components $E_p^{k,\nu}(t)$ on the dynamical variables $Q_p^{k,\nu}$; see Eq. (7). For the Fourier component with frequency ω and wave vector $\mathbf{q}$ this yields, in matrix form,

$$\underline{h}(\mathbf{q},\omega)=-\underline{Q}\,\underline{E}(\mathbf{q},\omega)\ , \tag{B4}$$

where the matrix $\underline{Q}$ is given by Eq. (16). When the response of the system is also expressed in terms of the dynamical variables

$$\underline{Y}(\mathbf{q},\omega)=\tilde{\underline{Q}}^{\,T}\underline{\delta}(\mathbf{q},\omega) \tag{B5}$$

and the generalized susceptibility $\underline{\chi}(\mathbf{q},\omega)$ is defined by

$$\underline{Y}(\mathbf{q},\omega)=\underline{\chi}(\mathbf{q},\omega)\underline{E}(\mathbf{q},\omega) \tag{B6}$$

then it follows from Eq. (B3) that

$$\underline{\chi}(\mathbf{q},\omega)=\tilde{\underline{Q}}^{\,T}[\omega-\underline{M}(\mathbf{q})]^{-1}\underline{P}\,\underline{Q}\ . \tag{B7}$$

The TDH (de)excitation energies of the system, i.e., the eigenvalues of the matrix $\underline{M}(\mathbf{q})$, correspond with the poles of the susceptibility $\underline{\chi}(\mathbf{q},\omega)$. Analogously, we define the MF single-particle susceptibility by

$$\underline{\chi}^{(0)}(\omega)=\tilde{\underline{Q}}^{\,T}(\omega-\underline{\varepsilon})^{-1}\underline{P}\,\underline{Q}\ , \tag{B8}$$

where the matrix $\underline{\varepsilon}$ contains the MF (de)excitation energies; see Eq. (14). If we insert Eq. (13) for $\underline{M}(\mathbf{q})$ into the linear-response equation (B3), multiply the latter by $\tilde{\underline{Q}}^{\,T}(\omega-\underline{\varepsilon})^{-1}$ and substitute Eqs. (B4), (B5), and (B8) we obtain

$$[\underline{I}+\underline{\chi}^{(0)}(\omega)\underline{W}(\mathbf{q})]\underline{Y}(\mathbf{q},\omega)=\underline{\chi}^{(0)}(\omega)\underline{E}(\mathbf{q},\omega)\ . \tag{B9}$$

Comparing this result with Eq. (B6) we find that the relation between the collective TDH susceptibility $\underline{\chi}(\mathbf{q},\omega)$ and the single-particle MF susceptibility $\underline{\chi}^{(0)}(\omega)$ is given by the Dyson equation, Eq. (20).

In considerations about orientational order-disorder phase transitions[42,43] the rotational MF Hamiltonians are replaced by free-rotor Hamiltonians, with well-known eigenstates. The rotational single-particle susceptibility $\underline{\chi}^{(0)}(\omega)$ can then be evaluated relatively simply, in some models even analytically. The translational susceptibility is usually approximated by the analytical formula for harmonic oscillators. At higher temperatures, these susceptibilities are sometimes calculated within the classical approximation.[42] Cubic and quartic terms in the lattice Hamiltonian, Eq. (8), are neglected and only the lowest-order dynamical variables for the rotations, see Eq. (7), are retained. This yields a simplified coupling matrix $\underline{W}(\mathbf{q})$ which does not depend on averaged dynamical variables as occurring in Eq. (18). In our calculations we avoid such approximations. The accuracy to which Eq. (20) is equivalent to TDH is only limited by the use of a finite basis.

[1]T. T. Chung and J. G. Dash, Surf. Sci. **66**, 559 (1977).
[2]A. D. Migone, H. K. Kim, M. H. W. Chan, J. Talbot, D. J. Tildesley, and W. A. Steele, Phys. Rev. Lett. **51**, 192 (1983).
[3]Q. M. Zhang, H. K. Kim, and M. H. W. Chan, Phys. Rev. B **33**, 413 (1986).
[4]Q. M. Zhang, H. K. Kim, and M. H. W. Chan, Phys. Rev. B **32**, 1820 (1985).
[5]Y. Larher, J. Chem. Phys. **68**, 2257 (1978).
[6]R. D. Diehl and S. C. Fain, Surf. Sci. **125**, 116 (1983).
[7]J. K. Kjems, L. Passell, H. Taub, J. G. Dash, and A. D. Novaco, Phys. Rev. B **13**, 1446 (1976).
[8]J. Eckert, W. D. Ellenson, J. B. Hastings, and L. Passell, Phys. Rev. Lett. **43**, 1329 (1979).
[9]R. Wang, S. K. Wang, H. Taub, J. C. Newton, and H. Schechter, Phys. Rev. B **35**, 5841 (1987).
[10]S. K. Wang, J. C. Newton, R. Wang, H. Taub, J. R. Dennison, and H. Schechter, Phys. Rev. B **39**, 10 331 (1989).
[11]K. Morishige, C. Mowforth, and R. K. Thomas, Surf. Sci. **151**, 289 (1985).
[12]M. Nielsen, K. Kjaer, J. Bohr, and J. P. McTague, J. Electron Spectrosc. Relat. Phenom. **30**, 111 (1983).
[13]V. L. P. Frank, H. J. Lauter, and P. Leiderer, in *Phonons 89,* edited by S. Hunklinger *et al.* (World Scientific, Singapore, 1990), p. 913.
[14]V. L. P. Frank, H. J. Lauter, F. Y. Yansen, H. Taub, L. W. Bruch, and J. R. Dennison, in *Phonons 89,* edited by S. Hunklinger *et al.* (World Scientific, Singapore, 1990), p. 922.
[15]F. Y. Hansen, V. L. P. Frank, H. Taub, L. W. Bruch, H. J. Lauter, and J. R. Dennison, Phys. Rev. Lett. **64**, 764 (1990).
[16]K. B. Gibson, S. J. Sibener, B. M. Hall, D. L. Mills, and J. E. Black, J. Chem. Phys. **83**, 4256 (1985).
[17]D. Eichenauer, U. Harten, J. P. Toennies, and V. Celli, J. Chem. Phys. **86**, 3693 (1987).
[18]K. Kern and G. Comsa, Adv. Chem. Phys. **76**, 211 (1989).
[19]L. W. Bruch, J. Chem. Phys. **79**, 3148 (1983).
[20]C. R. Fuselier, N. S. Gillis, and J. C. Raich, Solid State Commun. **25**, 747 (1978).
[21]G. Cardini and S. F. O'Shea, Surf. Sci. **154**, 231 (1985).
[22]D. J. Tildesley and R. M. Lynden-Bell, J. Chem. Soc. Faraday Trans. 2 **82**, 1605 (1986).
[23]S. E. Roosevelt and L. W. Bruch, Phys. Rev. B **41**, 12 236 (1990).
[24]B. Kuchta and R. D. Etters, Phys. Rev. B **36**, 3400 (1987).
[25]B. Kuchta and R. D. Etters, Phys. Rev. B **36**, 3407 (1987).
[26]B. Kuchta and R. D. Etters, J. Chem. Phys. **88**, 2793 (1988).
[27]C. Peters and M. L. Klein, Phys. Rev. B **32**, 6077 (1985).
[28]C. Peters and M. L. Klein, Mol. Phys. **54**, 895 (1985).
[29]Y. P. Yoshi and D. J. Tildesley, Mol. Phys. **55**, 999 (1985).
[30]J. Talbot, D. J. Tildesley, and W. A. Steele, Mol. Phys. **51**, 1331 (1984).
[31]J. Talbot, D. J. Tildesley, and W. A. Steele, Surf. Sci. **169**, 71 (1986).
[32]H. You and S. C. Fain, Faraday Discuss. Chem. Soc. (London) **80**, 159 (1985).
[33]R. M. Berns and A. van der Avoird, J. Chem. Phys. **72**, 6107 (1980).
[34]A. van der Avoird, P. E. S. Wormer, F. Mulder, and R. Berns, Topics Curr. Chem. **93**, 1 (1980).
[35]A. P. J. Jansen, W. J. Briels, and A. van der Avoird, J. Chem. Phys. **81**, 3648 (1984).
[36]A. van der Avoird, W. J. Briels, and A. P. J. Jansen, J. Chem. Phys. **81**, 3658 (1984).
[37]W. J. Briels, A. P. J. Jansen, and A. van der Avoird, J. Chem. Phys. **81**, 4118 (1984).
[38]A. P. J. Jansen and R. Schoorl, Phys. Rev. B **38**, 11 711 (1988).
[39]T. H. M. van den Berg, M. M. G. Bongers, and A. van der Avoird, J. Phys. Condens. Matter **2**, 8015 (1990).
[40]W. A. Steele, J. Phys. (Paris) Colloq. **38**, C4-61 (1978).
[41]D. R. Fredkin and N. R. Werthamer, Phys. Rev. A **138**, 1527 (1965).
[42]J. C. Raich, H. Yasuda, and E. R. Bernstein, J. Chem. Phys. **78**, 6209 (1983).
[43]B. de Raedt and K. H. Michel, Phys. Rev. B **19**, 767 (1979).
[44]D. N. Zubarev, *Nonequilibrium Statistical Thermodynamics* (Consultants Bureau, New York, 1974).
[45]T. H. M. van den Berg and A. van der Avoird, Phys. Rev. B **40**, 1932 (1989).
[46]D. A. Goodings and H. Henkelman, Can. J. Phys. **49**, 2898 (1971).
[47]J. K. Kjems and G. Dolling, Phys. Rev. B **11**, 1639 (1975).
[48]B. C. Kohin, J. Chem. Phys. **33**, 882 (1960).
[49]D. M. Brink and G. R. Satchler, *Angular Momentum* (Clarendon, Oxford, 1975).
[50]W. A. Steele, Surf. Sci. **36**, 317 (1973).
[51]R. D. Diehl and S. C. Fain, J. Chem. Phys. **77**, 5065 (1982).
[52]R. D. Diehl and S. C. Fain, Phys. Rev. B **26**, 4785 (1982).
[53]A. R. Edmonds, *Angular Momentum in Quantum Mechanics* (Princeton University Press, Princeton, NJ, 1957).
[54]K. G. Kay, H. D. Todd, and H. J. Silverstone, J. Chem. Phys. **51**, 2359 (1969).